Organic LETTERS

Letter

pubs.acs.org/OrgLett

Acetylcholinesterase-Capped Mesoporous Silica Nanoparticles That Open in the Presence of Diisopropylfluorophosphate (a Sarin or Soman Simulant)

Lluís Pascual,[†,‡,§] Sameh El Sayed,[⊥] Ramón Martínez-Máñez,[*,†,‡,§] Ana M. Costero,[†,§,∥] Salvador Gil,[†,§,∥] Pablo Gaviña,[†,§,∥] and Félix Sancenón[*,†,‡,§]

[†]Instituto Interuniversitario de Investigación de Reconocimiento Molecular y Desarrollo Tecnológico (IDM), Universitat Politècnica de València, Universitat de Valencia, 46022 Valencia, Spain

[‡]Departamento de Química, Universitat Politècnica de València, Camino de Vera s/n, 46022, Valencia, Spain

[§]CIBER de Bioingeniería, Biomateriales y Nanomedicina (CIBER-BBN)

[⊥]Dipartimento di Chimica, Università di Pavia, via Taramelli 12, I-27100 Pavia, Italy

[∥]Departamento de Química Orgánica, Universitat de València, Doctor Moliner 50, Burjassot, 46100 Valencia, Spain

Supporting Information

ABSTRACT: Mesoporous silica nanoparticles loaded with rhodamine B and capped with acetylcholinesterase are able to be selectively opened and deliver their cargo in the presence of nerve agent simulant diisopropyl fluorophosphate (DFP).

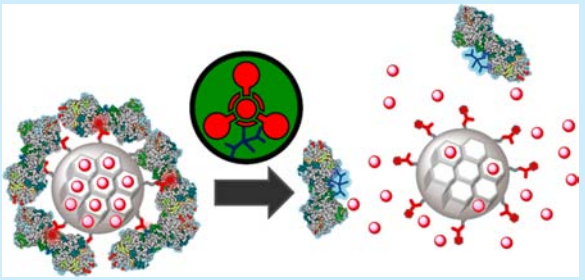

Nowadays, unfortunately, nerve agents have become a matter of concern for our society. Their use as chemical weapons in indiscriminate attacks carried out by terrorists and in armed conflicts boosted the interest of the international community on these lethal molecules.[1,2] Nerve agents are hazardous species because they can disrupt certain functions of the nervous system.[3−5] In this respect, nerve agents are known to cause severe toxicity because are able to inhibit acetylcholinesterase enzyme with the subsequent accumulation of acetylcholine in synaptic junctions, hindering muscle relaxation.[6] In addition, nerve agents are easily synthesized, and their indiscriminate use by terrorist organizations has directed interest toward remediation and detection studies of these lethal chemicals.[7−13]

The preparation of smart nanodevices based on mesoporous silica scaffolds (in the form of micro- or nanoparticles) has attracted much attention in recent years.[14−18] Mesoporous silicas present interesting features such as large surface area, inertness, ease of functionalization using well-known alkoxysilane chemistries, and the presence of a highly ordered porous network.[19] One recently developed appealing concept that uses mesoporous scaffolds is the design of gated mesoporous materials. To prepare these gated systems, the pores of the inorganic scaffold are loaded with selected cargoes, and the external surface is functionalized with certain (bio)molecules or supramolecular ensembles able to control the release of entrapped species upon application of triggering stimuli. These gated materials have been extensively used for the controlled release of drugs[20−24] and, more recently, in sensing and diagnostic applications.[25−31]

In relation to nerve agents, the use of gated mesoporous supports is especially appealing, and for instance, the design of capped solids able to be selectively opened in the presence of a certain nerve agent in an aqueous environment can be envisioned. Such devices have not been developed, but applications may be found, for instance, in remediation protocols (via the delivery of molecules able to hydrolyze nerve agents),[32,33] as early detection systems (releasing a reporter in the presence of nerve agents),[34] or in the release of a certain antidote.

In order to design such delivery systems that are capable of being selectively opened in the presence of certain nerve agents, we focused herein on the use of mesoporous silica materials and enzymes. Enzymes are highly valuable molecules as they have proven to have exquisite selectivity in the design of advanced gated devices for on-command delivery applications.[23,35−40] In fact, several enzyme-driven capped materials have been recently described, applied mainly for controlled release protocols in which a given cap is hydrolyzed in the presence of a certain enzyme.[15] In contrast, there are very few examples in which enzymes themselves are used as caps.[41]

Received: September 16, 2016
Published: October 18, 2016

DOI: 10.1021/acs.orglett.6b02793
Org. Lett. 2016, 18, 5548−5551

Based on these concepts, we report herein the preparation of mesoporous silica nanoparticles (MSNs) capable of selectively opening and releasing an entrapped cargo (we selected a dye as a proof of concept) in the presence of DFP, which is a mimic of nerve agents sarin or soman. We employed acetylcholinesterase (AChE) enzyme as the cap and rhodamine B as the cargo and directed experiments to detect DFP in aqueous environments. The design of the system is shown in Scheme 1. MSNs were first

Scheme 1. Schematic Representation of the Sensing Paradigm for DFP Detection Using Solid S1-AChE

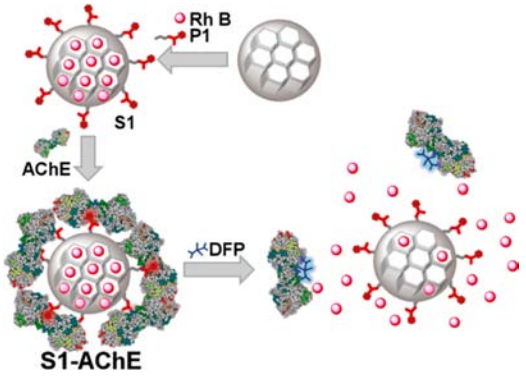

loaded with the rhodamine B dye, and the surface was grafted with **P1**, a derivative of pyridostigmine, which is a well-known AChE inhibitor.[6] The interaction between **P1** and AChE was expected to block pores and avoid the entrapped dye from leaking. We speculated that the presence of a stronger AChE inhibitor, such as DFP, would induce a displacement of the enzyme from the solid surface and result in cargo release (see Scheme 1).

MSNs were synthesized according to reported procedures.[42] The pores of the calcined mesoporous scaffold were loaded with fluorophore rhodamine B. In another step, the external surface of nanoparticles was functionalized with pyridostigmine derivative **P1** to yield solid **S1**. **P1** was obtained by a two-step procedure (see Scheme 2). In a first step, **1a** was reacted with **1b** to yield carbamate derivative **1c**. In a second step, the pyridine moiety in **1c** was quaternized upon the reaction with methyl iodide to yield **P1** (see the Supporting Information for further details). The final

Scheme 2. (A) Structure of the AChE Inhibitor Pyridostigimine and Synthesis of P1. (B) Chemical Structure of Nerve Agent Simulants and Other Organophosphorus Derivatives Tested

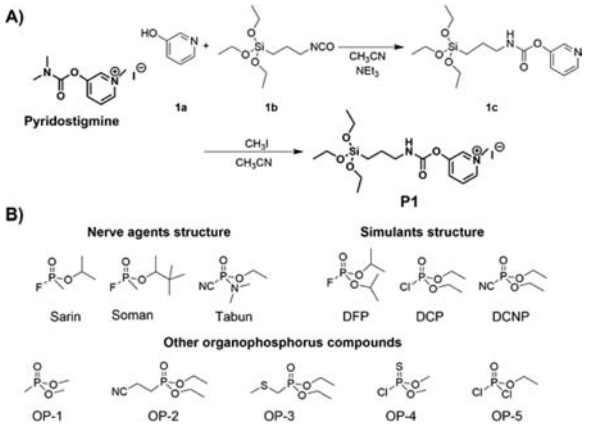

solid, **S1-AChE**, was prepared by suspending **S1** in an aqueous solution of AChE (TRIS buffer at pH 8.0) for 30 min (see the SI). UV−vis studies of the solution before and after the capping process allowed us to estimate that an amount of 250 ± 40 μmol g^{-1} AChE was attached to the final solid.

The starting MSNs and solid **S1** were characterized following standard procedures (see the SI for details). Powder X-ray diffraction (PXRD) and transmission electron microscopy (TEM), carried out on the starting MSNs, clearly showed the presence of a mesoporous structure that persisted in solid **S1** regardless of the loading process with rhodamine B and further functionalization with **P1** (see Figure 1). From the thermogravi-

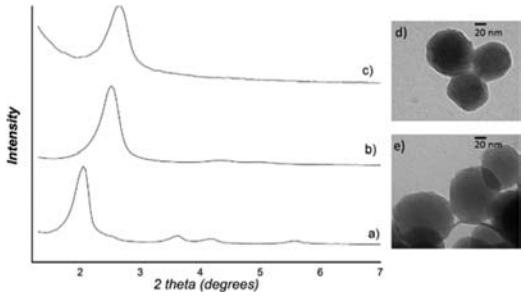

Figure 1. (Left) Powder X-ray patterns of (a) MCM-41 as synthesized; (b) calcined MCM-41; (c) solid **S1**. (Right) TEM images of (d) calcined MCM-41 and (e) solid **S1**.

metric and elemental analyses, rhodamine B (0.012 mmol/g SiO_2) and **P1** (0.93 mmol/g SiO_2) contents were determined. Table 1 lists the main structural properties (BET specific surface

Table 1. BET-Specific Surface Values, Pore Volumes, And Pore Sizes Calculated from the N_2 Adsorption−Desorption Isotherms

solid	S_{BET} (m^2 g^{-1})	BJH pore size[ac] (nm)	total pore volume[b] (cm^3 g^{-1})
MCM-41	747.5	2.45	0.334
S1	65.9		0.027

[a]Pore size was estimated by the BJH model, applied to the adsorption branch of the isotherm. [b,c]Pore volumes and pore sizes were associated with only intraparticle mesopores.

area, pore volumes, and pore sizes) for the starting MSNs and **S1** obtained from the N_2 adsorption−desorption measurements (see the SI for N_2 adsorption−desorption isotherms for calcined MCM-41 and **S1** and pore size distribution of calcined MCM-41 nanoparticles). The size of MSNs was assessed by TEM images, which gave an average particle diameter of 100 ± 8 nm (see Figure 1).

The activity of AChE in **S1-AChE** was measured using the Elman assay and amounted to 1.97 U mg^{-1} (see the SI for details). Remarkably, the activity of the enzyme in **S1-AChE** was significantly reduced when compared to the free enzyme (101.41 U mg^{-1}) due to the coordination of the enzyme active site with the **P1** inhibitor.

In a typical experiment, **S1-AChE** (500 μg) was suspended in TRIS buffer, and the resulting suspension was divided into two parts. Both mixtures were diluted with TRIS until a final volume of 1 mL. Then 3 μL of DFP or water was added to the suspensions. In both cases, the suspensions were stirred at room temperature, aliquots were extracted at certain times, and the solid was removed by centrifugation. Dye delivery to the bulk

DOI: 10.1021/acs.orglett.6b02793
Org. Lett. 2016, 18, 5548−5551

solution was easily detected by monitoring the emission band of rhodamine B at 572 nm upon excitation at 555 nm. The cargo release profile is shown in Figure 2. It can be seen that, in the

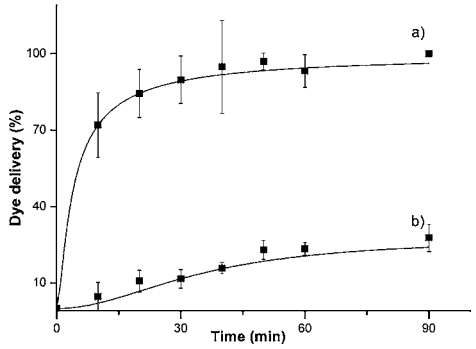

Figure 2. Kinetics of the release of rhodamine B from solid **S1-AChE** (a) in the presence of DFP and (b) in the absence of DFP.

absence of DFP, a poor rhodamine B release was found. However, when DFP was present, a remarkable cargo delivery was observed. The release of the entrapped rhodamine B was attributed to a preferential coordination of DFP with the active site of AChE enzyme. In fact, it has been reported that DFP displays a stronger interaction with the AChE enzyme (half the maximal inhibitory concentration (IC_{50}) for DFP is 120 nM)[43] than that shown by pyridostigmine derivative **P1** (IC_{50} for pyridostigmine is 330 nM).[44] Moreover, the partial delivery of rhodamine B observed in the absence of DFP was ascribed to the fact that **P1** (as pyridostigmine) is a reversible inhibitor of AChE enzyme. As a consequence, a slow enzymatic hydrolysis of **P1** occurs with subsequent detachment of enzyme from the surface and dye release.

Cargo release from **S1-AChE**, in the absence and in the presence of DFP, was monitored at pH 8.0 because this is the optimal proton concentration for the AChE enzyme. However, following a similar procedure, cargo release from **S1-AChE** was also studied at pH 4.0 and 6.0 (see the SI). Cargo release profiles at these pHs were quite similar to that found at pH 8.0. However, at pH 4.0 and 6.0, in the absence of DFP, a greater pore closure was observed, and in the presence of DFP, the release of rhodamine B was reduced at short times when compared with the delivery profiles at pH 8. These observations are most likely due to the lower AChE enzymatic activity at acidic pH.

To assess the selective aperture of **S1-AChE** with DFP, the fluorogenic response of **S1-AChE** in the presence of other nerve agent simulants and some other organophosphorus compounds was tested (see Scheme 2 for chemical structures). Figure 3 shows the emission of rhodamine B in the solution at 572 nm 15 min after addition of these organophosphorous derivatives (1000 ppm) to the buffered suspensions of **S1-AChE**. It is apparent from Figure 3 that **S1-AChE** is highly selective for DFP, whereas other simulants such as DCP, DCNP, and other organophosphorous derivatives such as OP1-OP5 were unable to induce remarkable cargo delivery.

In order to test sensitivity in terms of the cargo release of **S1-AChE** for DFP, the fluorogenic response obtained upon the addition of increasing quantities of this nerve agent simulant (after 15 min) was tested. As seen in Figure 4, a clear correlation between DFP concentration and rhodamine B release was observed, which agreed with an uncapping protocol that involved AChE displacement from the surface of MSNs. From the

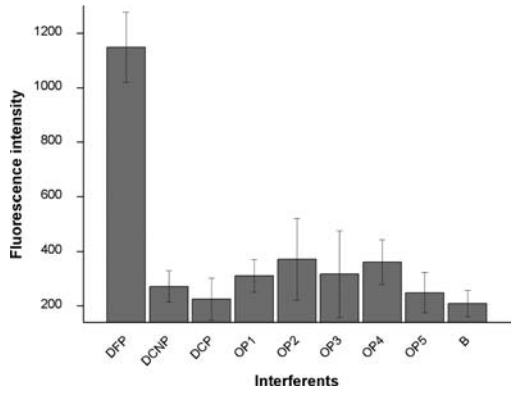

Figure 3. Emission intensity of rhodamine B at 572 nm (excitation at 555 nm) released from solid **S1-AChE** (TRIS, pH 8.0) in the presence of selected organophosphorous derivatives (1000 ppm) 15 min after addition.

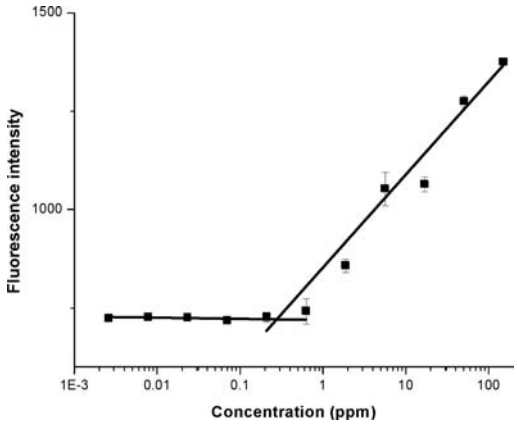

Figure 4. Release of rhodamine B from solid **S1-AChE** in the presence of different amounts of DFP in TRIS buffer at pH 8.0 15 min after addition.

titration profile shown in Figure 4, a limit of detection (LOD) for DFP as low as 0.28 ppm was determined.

Sensing features of **S1-AChE** for the detection of DFP in aqueous environments are similar to those of other reported probes (see the SI). **S1-AChE** displays a remarkable selectivity toward DFP and slower response time (15 min), when compared with other probes, which are in the range of few minutes (from 0.5 to 5). The slower response observed with **S1-AChE** was ascribed to several factors. In this respect, in order to detach AChE from the surface of the solid, DFP must first displace **P1**. Then, once the DFP−AChE pair is formed, the rhodamine dye must diffuse from the porous structure to the bulk solution. This multistep mechanism is slower than that in other probes reported in the literature. In addition, the LOD of other published chemosensors ranged from 21 ppt to 147 ppm with the measured for **S1-AChE** nanoparticles (0.28 ppm) located in the lower part of the interval.

Finally, in order to assess the use of **S1-AChE** for DFP detection in a more realistic setting, we measured cargo release profiles from **S1-AChE** in tap water (pH 7.65, 637 μS cm^{-1}) in the absence and in the presence of DFP (3 μL). The obtained profiles were quite similar to those found in buffered solutions (see the SI) pointing toward a possible use of **S1-AChE** solid for the detection of DFP in real competitive media.

In summary, we report herein the synthesis, characterization, and delivery behavior of a new hybrid material functionalized

DOI: 10.1021/acs.orglett.6b02793
Org. Lett. 2016, 18, 5548−5551

with a pyridostigmine derivative and capped with AChE. The gated support is only able to open and deliver the cargo in the presence of nerve agent simulant DFP among other simulants and organophosphorous derivatives. As a proof of concept, we used this material for sensing DFP in aqueous solution by employing reporter rhodamine B as the cargo. The fluorogenic response obtained in the presence of DFP is a consequence of competitive DFP binding with the active site of the AChE, which resulted in cargo delivery. The response of capped nanoparticles is highly selective and sensitive to DFP with an LOD of 0.28 ppm.

■ ASSOCIATED CONTENT

Supporting Information

The Supporting Information is available free of charge on the ACS Publications website at DOI: 10.1021/acs.orglett.6b02793.

Synthesis and characterization of prepared nanoparticles and **P1**; controlled release experiments (PDF)

■ AUTHOR INFORMATION

Corresponding Authors

*E-mail: rmaez@qim.upv.es.
*E-mail: fsanceno@upvnet.upv.es.

Notes

The authors declare no competing financial interest.

■ ACKNOWLEDGMENTS

Financial support from the Spanish Government and FEDER funds (Project MAT2015-64139-C4-1) and the Generalitat Valenciana (Project PROMETEOII/2014/047) is gratefully acknowledged. L.P. is grateful to the Universitat Politécnica de Valencia for his grant.

■ REFERENCES

(1) Kelle, A. *Int. Aff.* **2013**, *89*, 143.
(2) Cardoza Zúñiga, R. *Anu. Colomb. Derecho Int.* **2015**, *8*, 17.
(3) Wheelis, M. *Pure Appl. Chem.* **2002**, *74*, 2247.
(4) Augerson, W. S. *Chem. Biol. Warf. Agents* **2000**, 99.
(5) *Chemical Warfare Agents*; Somani, S. M., Ed,; Academic Press: London, 1992.
(6) Rang, H. P.; Dale, M.; Ritter, J. M.; Flower, R. J.; Henderson, G. *Rang & Dale's Pharmacology*, 8th ed.; Elsevier Churchill Livingstone: London, 2015.
(7) Ajami, D.; Rebek, J. *Org. Biomol. Chem.* **2013**, *11*, 3936.
(8) El Sayed, S.; Pascual, L.; Agostini, A.; Martínez-Máñez, R.; Sancenón, F.; Costero, A. M.; Parra, M.; Gil, S. *ChemistryOpen* **2014**, *3*, 142.
(9) Eubanks, L. M.; Dickerson, T. J.; Janda, K. D. *Chem. Soc. Rev.* **2007**, *36*, 458.
(10) Hiscock, J. R.; Sambrook, M. R.; Wells, N. J.; Gale, P. A. *Chem. Sci.* **2015**, *6*, 5680.
(11) Singh, V. V.; Wang, J. *Nanoscale* **2015**, *7*, 19377.
(12) Smith, B. M. *Chem. Soc. Rev.* **2008**, *37*, 470.
(13) Pascual, L.; Campos, I.; Bataller, R.; Olguín, C.; García-Breijo, E.; Martínez-Mañez, R.; Soto, J. *Sens. Actuators, B* **2014**, *192*, 134.
(14) Alberti, S.; Soler-Illia, G. J. A. A.; Azzaroni, O. *Chem. Commun.* **2015**, *51*, 6050.
(15) Aznar, E.; Oroval, M.; Pascual, L.; Murguía, J. R.; Martínez-Máñez, R.; Sancenón, F. *Chem. Rev.* **2016**, *116*, 561.
(16) Li, Z.; Barnes, J. C.; Bosoy, A.; Stoddart, J. F.; Zink, J. I. *Chem. Soc. Rev.* **2012**, *41*, 2590.
(17) Lu, C.-H.; Willner, I. *Angew. Chem., Int. Ed.* **2015**, *54*, 12212.
(18) Slowing, I. I.; Trewyn, B. G.; Giri, S.; Lin, V. S. -Y. *Adv. Funct. Mater.* **2007**, *17*, 1225.
(19) Rurack, K.; Martínez-Mánez, R. *The Supramolecular Chemistry of Organic−Inorganic Hybrid Materials*; Wiley-VCH, 2010.
(20) Lee, J.; Kim, H.; Kim, S.; Lee, H.; Kim, J.; Kim, N.; Park, H. J.; Choi, E. K.; Lee, J. S.; Kim, C. *J. Mater. Chem.* **2012**, *22*, 14061.
(21) Torney, F.; Trewyn, B. G.; Lin, V. S. -Y.; Wang, K. *Nat. Nanotechnol.* **2007**, *2*, 295.
(22) Mal, N. K.; Fujiwara, M.; Tanaka, Y. *Nature* **2003**, *421*, 350.
(23) Agostini, A.; Mondragon, L.; Bernardos, A.; Martínez-Mañez, R.; Marcos, M. D.; Sancenón, F.; Soto, J.; Costero, A. M.; Manguan-Garcia, C.; Perona, R.; Moreno-Torres, M.; Aparicio-Sanchis, R.; Murguía, J. R. *Angew. Chem., Int. Ed.* **2012**, *51*, 10556.
(24) Meng, H. A.; Xue, M.; Xia, T. A.; Zhao, Y. L.; Tamanoi, F.; Stoddart, J. F.; Zink, J. I.; Nel, A. E. *J. Am. Chem. Soc.* **2010**, *132*, 12690.
(25) (a) Sancenón, F.; Pascual, L.; Oroval, M.; Aznar, E.; Martínez-Mañez, R. *ChemistryOpen* **2015**, *4*, 418. (b) Aznar, E.; Martínez-Máñez, R.; Sancenón, F. *Expert Opin. Drug Delivery* **2009**, *6*, 643. (c) Tang, D.; Lin, Y.; Zhou, Q.; Lin, Y.; Li, P.; Niessner, R.; Knopp, D. *Anal. Chem.* **2014**, *86*, 11451.
(26) Zhao, Y. N.; Trewyn, B. G.; Slowing, I. I.; Lin, V. S. -Y. *J. Am. Chem. Soc.* **2009**, *131*, 8398.
(27) Climent, E.; Mondragon, L.; Martínez-Mañez, R.; Sancenón, F.; Marcos, M. D.; Murguía, J. R.; Amoros, P.; Rurack, K.; Perez-Paya, E. *Angew. Chem., Int. Ed.* **2013**, *52*, 8938.
(28) Zhang, Z. X.; Balogh, D.; Wang, F. A.; Willner, I. *J. Am. Chem. Soc.* **2013**, *135*, 1934.
(29) Hernandez, F. J.; Hernandez, L. I.; Pinto, A.; Schafer, T.; Ozalp, V. C. *Chem. Commun.* **2013**, *49*, 1285.
(30) Salinas, Y.; Martínez-Máñez, R.; Jeppesen, J. O.; Petersen, L. H.; Sancenón, F.; Marcos, M. D.; Soto, J.; Guillem, C.; Amoros, P. *ACS Appl. Mater. Interfaces* **2013**, *5*, 1538.
(31) Oroval, M.; Climent, E.; Coll, C.; Eritja, R.; Avino, A.; Marcos, M. D.; Sancenón, F.; Martínez-Máñez, R.; Amoros, P. *Chem. Commun.* **2013**, *49*, 5480.
(32) Candel, I.; Marcos, M. D.; Martínez-Máñez, R.; Sancenón, F.; Costero, A. M.; Parra, M.; Gil, S.; Guillem, C.; Perez-Pla, F.; Amoros, P. *Microporous Mesoporous Mater.* **2015**, *217*, 30.
(33) Barba-Bon, A.; Martínez-Mañez, R.; Sancenón, F.; Costero, A. M.; Gil, S.; Perez-Pla, F.; Llopis, E. *J. Hazard. Mater.* **2015**, *298*, 73.
(34) Candel, I.; Bernardos, A.; Climent, E.; Marcos, M. D.; Martínez-Máñez, R.; Sancenón, F.; Soto, J.; Costero, A. M.; Gil, S.; Parra, M. *Chem. Commun.* **2011**, *47*, 8313.
(35) Agostini, A.; Mondragon, L.; Pascual, L.; Aznar, E.; Coll, C.; Martínez-Máñez, R.; Sancenón, F.; Soto, J.; Marcos, M. D.; Amoros, P.; Costero, A. M.; Parra, M.; Gil, S. *Langmuir* **2012**, *28*, 14766.
(36) Radhakrishnan, K.; Tripathy, J.; Gnanadhas, D. P.; Chakravortty, D.; Raichur, A. M. *RSC Adv.* **2014**, *4*, 45961.
(37) Park, C.; Kim, H.; Kim, S.; Kim, C. *J. Am. Chem. Soc.* **2009**, *131*, 16614.
(38) Villalonga, R.; Díez, P.; Sánchez, A.; Aznar, E.; Martínez-Máñez, R.; Pingarron, J. M. *Chem. - Eur. J.* **2013**, *19*, 7889.
(39) Coll, C.; Mondragon, L.; Martínez-Máñez, R.; Sancenón, F.; Marcos, M. D.; Soto, J.; Amoros, P.; Perez-Paya, E. *Angew. Chem., Int. Ed.* **2011**, *50*, 2138.
(40) Patel, K.; Angelos, S.; Dichtel, W. R.; Coskun, A.; Yang, Y. W.; Zink, J. I.; Stoddart, J. F. *J. Am. Chem. Soc.* **2008**, *130*, 2382.
(41) (a) Chen, M. J.; Huang, C. S.; He, C. S.; Zhu, W. P.; Xu, Y. F.; Lu, Y. F. *Chem. Commun.* **2012**, *48*, 9522. (b) Aznar, E.; Villalonga, R.; Giménez, C.; Sancenón, F.; Marcos, M. D.; Martínez-Máñez, R.; Díez, P.; Pingarrón, J. M.; Amorós, P. *Chem. Commun.* **2013**, *49*, 6391. (c) Díez, P.; Sánchez, A.; de la Torre, C.; Gamella, M.; Martínez-Ruíz, P.; Aznar, E.; Martínez-Máñez, R.; Pingarrón, J. M.; Villalonga, R. *ACS Appl. Mater. Interfaces* **2016**, *8*, 7657.
(42) Kresge, C. T.; Leonowicz, M. E.; Roth, W. J.; Vartuli, J. C.; Beck, J. S. *Nature* **1992**, *359*, 710.
(43) Chan, K.; Jensen, N.; O'Brien, P. J. O. *J. Appl. Toxicol.* **2008**, *28*, 608.
(44) Lorke, D. E.; Hasan, M. Y.; Nurulain, S. M.; Shafiullah, M.; Kuca, K.; Petroianu, G. A. *J. Appl. Toxicol.* **2011**, *31*, 515.

DOI: 10.1021/acs.orglett.6b02793
Org. Lett. 2016, 18, 5548−5551